THE BELL SYSTEM TECHNICAL JOURNAL
Vol. 51, No. 2, February, 1972
Printed in U.S.A.

Controlled Response of a Ceramic Microphone

By R. E. NICKELL and D. C. STICKLER

(Manuscript received May 17, 1971)

One of the electromechanical transducer candidates for the electronic telephone is a bilamellar piezoelectric ceramic. In order to meet the design template for transducer response in the acoustic band, 0.3 kHz–3.0 kHz, a controlled resonant condition must be introduced at the upper end of the spectrum.*

An analytical program, consisting of three complementary parts, was carried out in order to understand the phenomenology of the transducer/support system response to acoustic loading. The three parts are: (i) a simple direct variational model, used to generate parametric design information; (ii) an exact solution with a lumped mechanical model of the support structure, used to evaluate the effect of using different rubber materials in relation to the design goal; and (iii) a finite element modal survey of the system, used to determine the necessary design modifications and to expose deficiencies in the previous models.

I. INTRODUCTION

Several alternative designs are under consideration as transducer elements for the electronic telephone.[1] One of the leading candidates is a bilamellar piezoelectric ceramic plate consisting of two thin circular ceramic wafers that are electroded on both surfaces and cemented together.[2] The disks are joined with opposing polarity so that the flexural response of the assembly to applied acoustic loading results in additive voltage output.

The design objectives for the transducer response as a function of driving frequency are shown in Fig. 1.[3] The cross-hatched areas indicate the template within which the response should fall. Important characteristics of this template are: (*i*) the electrical output rolls off below 300 Hz in order to exclude low-frequency room noise; (*ii*) output is

* It has since been decided to eliminate rubber from the design and to replace the bilamellar transducer by a metal/ceramic combination.

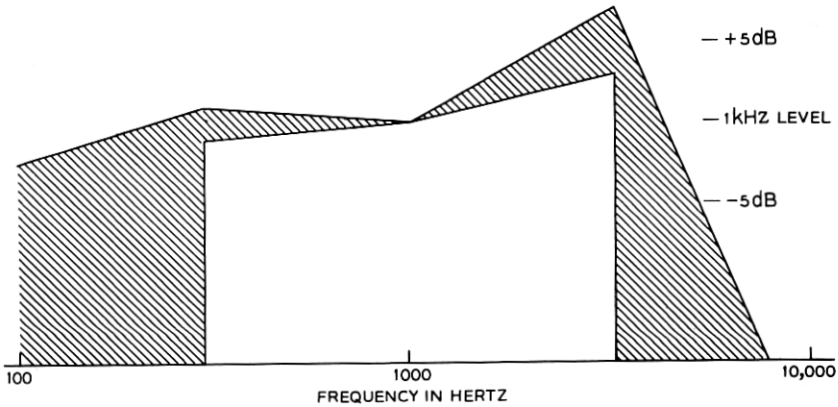

Fig. 1—Microphone response design objective.

relatively flat between 300 and 1000 Hz; (*iii*) output increases by approximately 7 dB between 1000 and 3000 Hz in order to compensate for transmission loop losses and to improve speech recognition; and (*iv*) output rolls off rapidly at frequencies above 3000 Hz in order to eliminate crosstalk and other high-frequency noise. The object of this investigation is to determine the extent to which transducer support damping can be used to achieve these characteristics while maximizing the microphone sensitivity.

The basic approach is to design a bilamellar structure with a fundamental flexural resonance near 3000 Hz—this will guarantee flat response up to frequencies just below the resonance—while providing a support configuration which will permit shaping the response around the resonant peak. In addition, this shaping should include the suppression of resonant response at higher frequencies. The shaping of the response curve at frequencies below 300 Hz is considered to be a manageable problem.

One support configuration that has been tried is shown in Fig. 2. The ceramic disks are mounted between soft rubber "O"-rings that are held in place by a relatively rigid housing. Such a design has one serious drawback—the lack of stability of the transducer response with respect to slight changes in rubber precompression. This sensitivity is due to the large contact area increase, and corresponding increase in support stiffness, as a function of slight changes in precompression. Large excursions in support stiffness will affect the location of the fundamental resonance and, thereby, distort the response.

A more dimensionally stable configuration is shown in Fig. 3. Conical

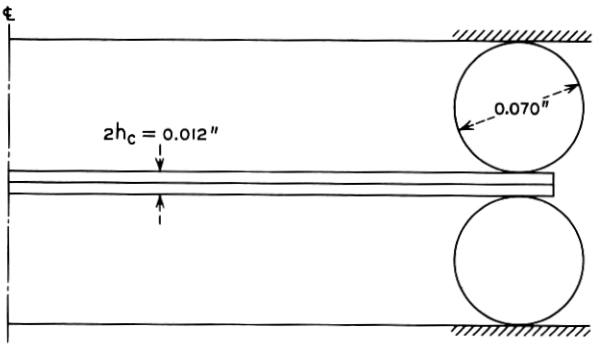

Fig. 2—"O"-ring support configuration.

rubber washers are placed above and below the disk and have flat surfaces in contact with the ceramic, insuring relatively constant stiffness with respect to precompression. The stiffness of the washer is primarily dependent on the thickness and height of the cross section, with a secondary dependence on the cone angle, shown as 25 degrees in Fig. 3. This design can be easily modified in order to achieve the response objectives by making suitable adjustments in these parameters.

While the concern here is with controlled response through support damping, other concepts, such as the addition of acoustic elements to the design (acoustic mass, compliance, and resistance) or constrained layer damping, could be considered.[3] Economic constraints are paramount in deciding the most feasible concept, however, so that manufacturability, material availability, and unit cost are vital ingredients.

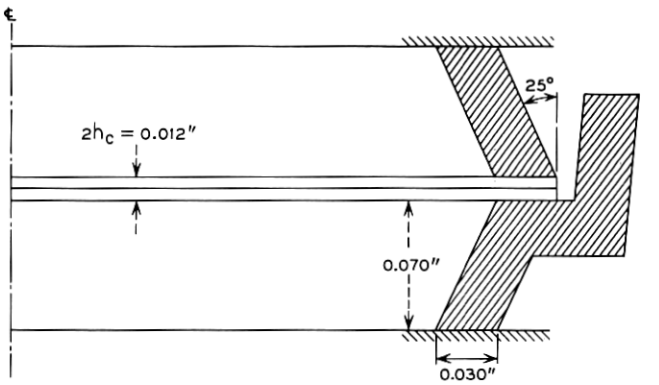

Fig. 3—Conical washer configuration.

In the following sections, an analytical effort that consists of three mutually complementary elements is described. First, a direct variational procedure is used to calculate, approximately, the first two resonant frequencies of the ceramic and its support system. The attraction of these approximate methods is their simplicity of expression and the consequent ease in assessing system trade-offs. The second phase deals with the washer as a lumped mechanical network that acts at an "effective support radius" and is accounted for by a boundary condition on the shear resultant at this location. The exact solution for the forced response of the transducer, as a function of driving frequency, is then found. The third phase consists of a resonant frequency and modal shape survey of the complete structure by using an elastic, axisymmetric, dynamic finite element code. These finite element results provide a check on previous calculations and give more detailed information on the motion executed by the support system.

From this description the role of analysis is seen to have several facets: (*i*) as a design guide (to identify parameters and to check initial experiments); (*ii*) as a key to understanding the phenomenology; (*iii*) to assess hard designs through detailed analysis; and (*iv*) to provide guidelines for future designs.

II. RUBBER CHARACTERISTICS

Before proceeding with the analytical details, a few comments on the thermomechanical properties of viscoelastic support materials are in order. From the transducer response template in Fig. 1, the primary information needed is the complex viscoelastic moduli over the frequency range 100 Hz–10,000 Hz. In addition, since the transducer must have stable response characteristics with respect to temperature changes down to about −40°C and up to about +50°C, the effect of temperature on these moduli must be known.

For these analyses, the candidate polymers were assumed to be isotropic, thus reducing the number of moduli about which knowledge is required down to two (e.g., the shear and bulk moduli). Also, it was assumed that the materials were nearly incompressible over the frequency and temperature ranges of interest (the bulk modulus much larger than the shear modulus), reducing the number down to one.[4] For example, if the complex extensional modulus is known, the complex shear modulus is found by dividing by three. It suffices, therefore, to know the storage modulus, in either extension or shear, and the loss tangent over the acoustic frequency range at temperatures in the environmental range.

An additional simplification is possible by assuming the polymers to be thermorheologically simple, so that the theory of reduced variables[5] applies (e.g., frequency and temperature are interrelated). Thus, if the complex extensional modulus as a function of circular frequency ω at a temperature T_o is given by ($i = \sqrt{-1}$)

$$E(\omega, T_o) = E'(\omega, T_o) + iE''(\omega, T_o), \tag{1}$$

where E' and E'' are the storage and loss moduli, respectively, then the extensional modulus at a temperature T is given by $E(\omega a_T, T_o)$. The multiplier a_T is referred to as the time-temperature shift function. For a typical polymer, such as polybutadiene, a plot of extensional modulus versus frequency (see Fig. 4) at room temperature can be used to generate data at other temperatures provided the shift function has been experimentally determined and provided that the room temperature data extends over a sufficient frequency range.

Characterizing each polymer to this extent is prohibitive, however, and the usual approach is to generate data at a fixed frequency while varying the temperature. Such data is shown in Fig. 5 for two polymers of interest: (*i*) a blend of 50 percent cis-4 polybutadiene and 50 percent styrene-butadiene rubber (called PBD/SBR) and (*ii*) a blend of 75 percent cis-4 polybutadiene and 25 percent chlorobutyl rubber (called PBD/CBT). A fixed frequency of 110 Hz (data obtained with a Vibron Viscoelastometer marketed by Imass, Inc., Accord, Mass.) was used and the temperature was varied sufficiently to capture the transition regions of interest.[6] Note that the loss tangent, defined by

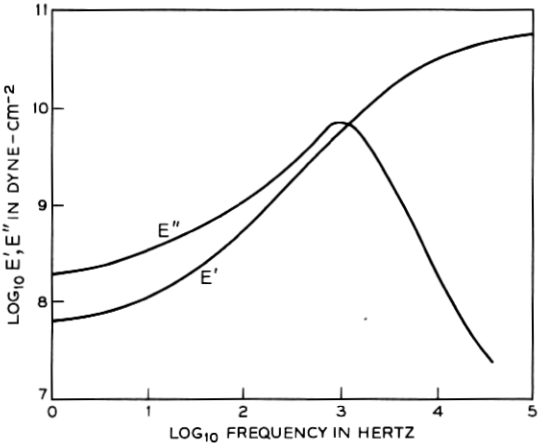

Fig. 4—Complex extensional modulus, polybutadiene, $T = 20°C$.

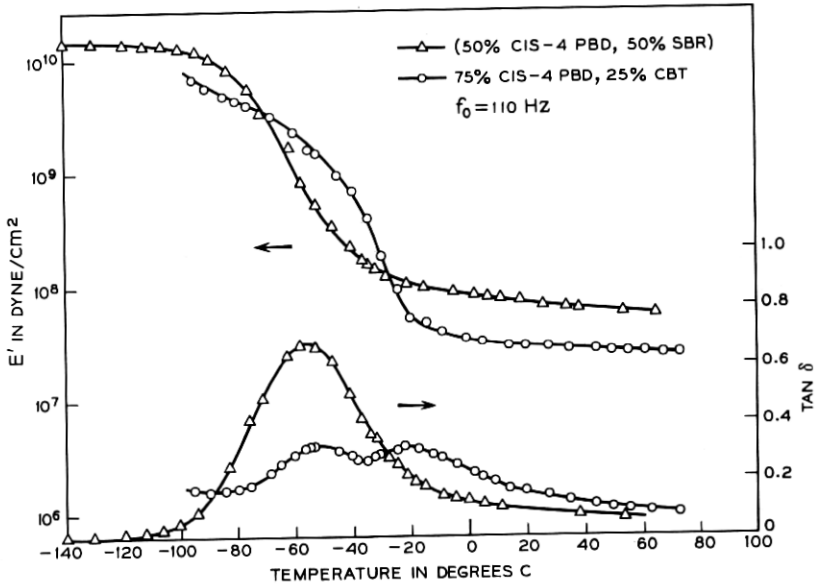

Fig. 5—E' and tan δ vs temperature.

$$\tan \delta = E''/E', \tag{2}$$

has been shown in lieu of the imaginary component of the modulus.

In order to construct modulus versus frequency from these data, the shift function for each polymer must be known. Ordinarily, a_T would be determined experimentally from several fixed frequency runs and their graphical superposition. It is often convenient, however, to assume a form for the shift function that is found to fit a wide variety of polymers and is called the WLF equation:[7]

$$\log_{10} a_T = -c_1(T - T_R)/(c_2 + T - T_R), \tag{3}$$

where c_1 and c_2 are constants and T_R is a reference temperature. Common practice is to use $c_1 = 8.86$ and $c_2 = 101.5$ as the constants and a reference temperature in the middle of the transition region. For the analytical work described here, T_R for the PBD/SBR was selected as -60°C and for the PBD/CBT was chosen as -40°C. Then, with the help of (3), the data of Fig. 5 was converted to the form of Fig. 4 for specific temperatures.

These modulus values can be approximately converted to effective stiffness by using simple strength of materials considerations. If the cone angle is neglected and the washer is assumed to be in a state

of plane stress, then the factor which converts modulus to stiffness (per radian) can be written

$$\kappa = \frac{2\bar{r}t}{l(1 - \nu_R^2)}, \tag{4}$$

where $\bar{r}$ is an average radius for the washer, t is its thickness, l is the height, ν_R is the Poisson's ratio for the rubber, and the multiplier indicates that both washers are being taken into account. The cantilever frustum, which does not provide support stiffness in its unconstrained configuration, is neglected. If ν_R is assumed to be 0.5 and the dimensions of Fig. 3 are used, $\kappa \doteq 0.8$, indicating that the effective rubber stiffness per radian is eight-tenths of the extensional modulus. This conversion factor will be used in the next section in order to help generate parametric design information.

III. SIMPLE VARIATIONAL SOLUTION

As a first step in the rational design process, a procedure for estimating the two lowest resonant frequencies of the transducer, as a function of geometric and material parameters, is developed. A Rayleigh–Ritz procedure is used for deriving these design equations. First, a functional is written which represents the strain energy and kinetic energy of the plate and its deformable supports, less the work done by the acoustic loading.[8] Classical infinitesimal plate theory is used (rotatory inertia and shear deformation are neglected) and piezoelectric stiffening effects are ignored. Then

$$\begin{aligned} F(w) = {} & \frac{1}{2}\int_0^{r_c} D(r)\left\{\left(\frac{\partial^2 w}{\partial r^2} + \frac{1}{r}\frac{\partial w}{\partial r}\right)^2 - 2(1-\nu)\left(\frac{\partial^2 w}{\partial r^2}\right)\left(\frac{1}{r}\frac{\partial w}{\partial r}\right)\right\} r dr \\ & - \tfrac{1}{2}\omega^2 \int_0^{r_c} \rho(r)h(r)\{w(r,t)\}^2 r dr - \int_0^{r_c} p(r,t)w(r,t) r dr \\ & + \tfrac{1}{2} r_s k_s \{w(r_s, t)\}^2 - \tfrac{1}{2}\omega^2 r_s M_s \{w(r_s, t)\}^2, \end{aligned} \tag{5}$$

where r is the radial coordinate of the circular plate, t is the time, and $w(r, t)$ is transverse deflection. The flexural stiffness, density, thickness, Poisson's ratio, and radius of the plate are $D(r)$, $\rho(r)$, $h(r)$, $\nu(r)$, and r_c, respectively. The effective mass, effective stiffness, and effective support radius for the rubber are denoted by M_s, k_s, and r_s, respectively. The circular frequency is ω and the applied acoustic pressure is $p(r, t)$.

Next, an approximate deflected shape is assumed, in terms of one

or more undetermined parameters, and substituted into (5). This shape function should satisfy the geometric boundary conditions for the plate (i.e., those on deflection and slope) identically, but may also satisfy natural boundary conditions (i.e., on shear and bending moment). After substitution, the spatial integration is carried out; then, the stationary value of the functional is found through the first variation and subsequent solution of simultaneous equations for the undetermined parameters. Eigenvalues are found from the homogeneous system. The procedure has been used for clamped and simply supported plates[9] and is usually found to be within a few percent of exact solutions.

The trial function for the microphone is taken to be

$$w(r) = \alpha_o + \alpha_1\left[1 - \left(\frac{6 + 2\nu}{5 + \nu}\right)\left(\frac{r}{r_c}\right)^2 + \left(\frac{1 + \nu}{5 + \nu}\right)\left(\frac{r}{r_c}\right)^4\right] \tag{6}$$

where α_o and α_1 are the undetermined parameters (the harmonic time dependence has been suppressed). This trial function has the properties that

$$w(0) = \alpha_o + \alpha_1 , \tag{7a}$$

$$w(r_c) = \alpha_o , \tag{7b}$$

and

$$M_r(r_c) = 0. \tag{7c}$$

This implies that the generalized coordinate α_o represents the motion at the outside edge of the plate and that the generalized coordinate α_1 represents motion of the center of the plate relative to edge motion. The boundary condition on shear at the outside edge is not, and need not be, satisfied by the trial function; the boundary condition or radial bending moment at the outside edge, which also need not be satisfied by the trial function, is explicitly satisfied, as indicated by (7c). Note that (6) has the value $w(r_s) = \bar{w}_s$ at the effective support radius.

Carrying out the steps previously indicated yields the matrix equation governing the system:

$$[[K] - \omega^2[M]]\begin{Bmatrix}\alpha_o \\ \alpha_1\end{Bmatrix} = \{F\}, \tag{8}$$

where the stiffness matrix, $[K]$; the mass matrix, $[M]$; and the load vector, $\{F\}$, are given by

$$[K] = \frac{D}{r_c^2}\begin{bmatrix} \lambda & \lambda\bar{w}_s \\ \lambda\bar{w}_s & \lambda\bar{w}_s^2 + \dfrac{32(1 + \nu)(7 + \nu)}{3(5 + \nu)^2} \end{bmatrix}, \tag{9a}$$

$$[M] = \rho h r_c^2 \begin{bmatrix} \frac{1}{2} + m & \frac{1}{6}\left(\frac{7+\nu}{5+\nu}\right) + m\bar{w}_s \\ \frac{1}{6}\left(\frac{7+\nu}{5+\nu}\right) + m\bar{w}_s & \frac{(3\nu^2 + 36\nu + 113)}{30(5+\nu)^2} + m\bar{w}_s^2 \end{bmatrix}, \tag{9b}$$

and

$$\{F\} = \tfrac{1}{2} p_0 r_l^2 \begin{Bmatrix} 1 \\ \left[1 - \left(\frac{3+\nu}{5+\nu}\right)\left(\frac{r_l}{r_c}\right)^2 + \frac{1}{3}\left(\frac{1+\nu}{5+\nu}\right)\left(\frac{r_l}{r_c}\right)^4\right] \end{Bmatrix}, \tag{9c}$$

respectively. The dimensionless parameters λ and m are defined by

$$\lambda = \frac{r_c^2 r_s k_s}{D}; \qquad m = \frac{r_s M_s}{\rho h r_c^2}; \tag{10}$$

and the variables p_0 and r_l are the uniform acoustic pressure and the loading radius ($0 < r_l < r_s$).

As an illustration of the Rayleigh–Ritz procedure, consider a transducer composed of two PZT-5A disks, each 0.006 inch thick and 0.590 inch in diameter. The bonding layer is assumed to have negligible thickness. With an in-plane extensional modulus of 6.1×10^{11} dynes/cm^2 and a Poisson's ratio of 0.35, the flexural stiffness for the plate is $D = 1.644 \times 10^6$ dyne-cm. The effective radius of the rubber support (the centerline of contact with the conical washer) is taken to be 0.708 cm, $r_c = 0.75$ cm, the density for PZT-5A is 7.8 g/cm^3, and the total thickness of the plate is 0.0305 cm.

Using these data, approximate values for the first two resonant frequencies can be found as a function of the stiffness ratio, λ, and the mass ratio, m. Figure 6 shows these two resonances plotted parametrically with respect to λ and m. From this plot, the primary effect of the rubber effective mass is to lower both resonances (the second much more markedly than the first).

The Rayleigh–Ritz results are summarized in Table I. Effective translational inertia is found from Ref. 10, where the effective mass of a rubber block bonded between two plates was shown to be slightly larger than one-third of the total mass. Since the total rubber volume per radian is 0.0312 cm^3 and $r_s = 0.708$ cm, then

$$M_s = 0.0146\ \rho_R \text{ g/cm/radian}, \tag{11}$$

where ρ_R is the density of the rubber ($\rho_R \doteq 1.2$ for PBD/SBR and 1.0 for PBD/CBT). The extensional modulus values are obtained by fitting the WLF shifted data of Fig. 5 by collocation;[11] the effective

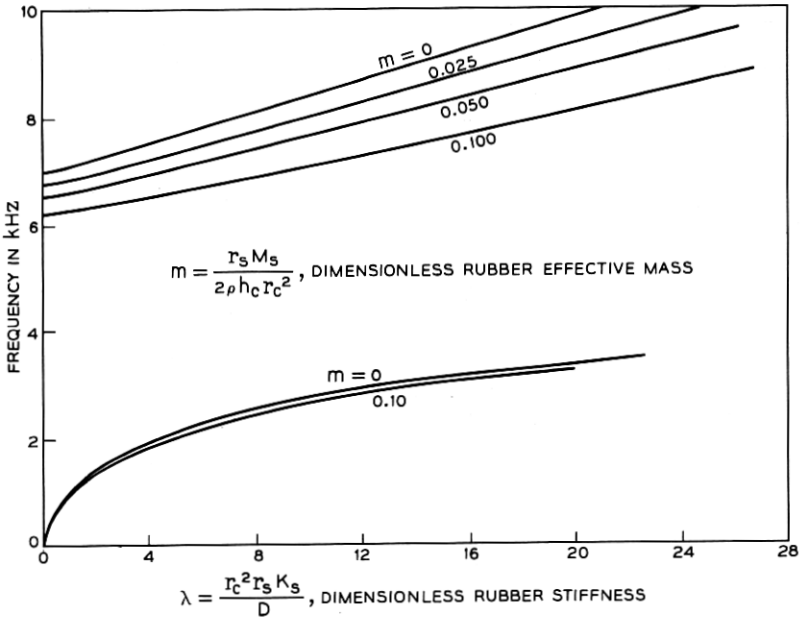

Fig. 6—First and second resonances vs rubber mass and stiffness.

stiffness is then computed using the conversion factor, $\kappa = 0.8$, found previously. The frequencies shown in Table I will be seen later to be in excellent agreement with measured results.

The direct variational calculations can be extended to include forced response and complex rubber properties. Rather than rely on (8) entirely, however, a more exact representation is formulated in the next section.

TABLE I—RAYLEIGH–RITZ RESULTS

	PBD/SBR		PBD/CBT	
	3 kHz	10 kHz	3 kHz	10 kHz
M_s	0.0176	0.0176	0.0146	0.0146
m	0.093	0.093	0.078	0.078
E	116×10^6	148×10^6	48×10^6	59×10^6
k_s	92×10^6	118×10^6	38×10^6	47×10^6
λ	22.5	28.5	9.5	11.5
f_1	3.3 kHz		2.7 kHz	
f_2	9.2 kHz		7.3 kHz	

IV. EXACT SOLUTION–LUMPED SUPPORT PARAMETERS

In this section, the effect of the support stiffness and damping is treated through a boundary condition on the shear resultant. This resultant is assumed to act at the mean radius of the conical washer, implying that the contact area of the rubber is small in comparison to the area of the ceramic (see Fig. 3). Then, the forced harmonic response of the plate can be found from the solution to

$$\nabla^4 w - k^4 w = \begin{cases} -\dfrac{p_o}{D} e^{i\omega t}, & 0 < r < r_l \\ 0, & r_l < r < r_c \end{cases} \tag{12}$$

where the wave number, k, is defined by

$$k^4 = \frac{\rho h \omega^2}{D}. \tag{13}$$

Due to the assumed cylindrical symmetry of the pressure, only axisymmetric solutions of (12) are sought. The plate is then divided into three regions: (*i*) $0 < r < r_l$; (*ii*) $r_l < r < r_s$; and (*iii*) $r_s < r < r_c$. Solutions over these regions are pieced together by satisfying continuity (boundary) conditions on the transverse displacement, the slope, the radial bending moment, and the shear force at the radii r_l and r_s ; in addition, the homogeneous boundary conditions on radial bending moment and shear at the free outer edge of the plate are satisfied. At the effective support radius,

$$Q(r_{s-}) - Q(r_{s+}) = [\omega^2 M_s - k_s(\omega)]w(r_s); \tag{14}$$

i.e., the net shear is opposed by a complex impedance that is proportional to the transverse displacement at that point. The impedance is composed of an inertia term, represented by $\omega^2 M_s$, and a complex stiffness, written as a generalized Maxwell model[12] in the form

$$k_s(\omega) = k_s'(\omega) + ik_s''(\omega), \tag{15}$$

where

$$k_s'(\omega) = k_R + \sum_{n=1}^{N} \frac{k_n \omega^2 \tau_n^2}{1 + \omega^2 \tau_n^2}, \tag{16a}$$

$$k_s''(\omega) = \sum_{n=1}^{N} \frac{k_n \omega \tau_n}{1 + \omega^2 \tau_n^2}, \tag{16b}$$

and k_R , k_n , and τ_n are the equilibrium (rubbery) stiffness, an incre-

mental stiffness, and a relaxation time associated with an incremental stiffness, respectively.

The technique that is used to solve this system, subject to the above stated boundary conditions, does not require the determination of the eigenfunctions of the problem. This procedure can be avoided since a particular solution is known: namely,

$$w_p = \begin{cases} \frac{p_o}{k^4 D}, & 0 < r < r_l \\ 0, & r_l < r < r_e . \end{cases} \tag{17}$$

To this solution it is necessary only to add properly weighted homogeneous solutions to satisfy the boundary conditions—in this case, ordinary and modified Bessel functions of zero order. The matrix inversion required to find the proper weights is carried out on a digital computer and the solution to (12) can then be determined as a function of the acoustic driving frequency. The voltage output is then found from the expression derived in the Appendix.

Two numerical examples are solved in order to illustrate the procedure and to compare the exact (lumped parameter) results with experiment. The transducer design is identical in both cases; the only difference is the conical washer material—in the first case, the PBD/SBR blend; in the second case, the PBD/CBT blend. Effective mass and stiffness are computed by procedures that were described previously. The comparison to experiment for the PBD/SBR blend is shown in Fig. 7 and a similar comparison for the PBD/CBT blend is shown in Fig. 8.

The response comparison for both examples is favorable up to frequencies slightly above the first resonance; then, in both cases, an intermediate response peak is not captured by this model and the response peak at the next resonance is predicted to be much lower than shown by experiment. The location of this latter peak is, however, quite favorable. Perhaps the most disturbing feature of the comparison is the encouraging proximity of the analytical results to the design goal (see Fig. 1)—encouragement that is not borne out by the actual transducer performance. It seems apparent that other deformation mechanisms, not represented adequately by the lumped mechanical model of the conical washer support, are dominating the response at the higher frequencies. For this reason, a more exact model of the support structure is in order.

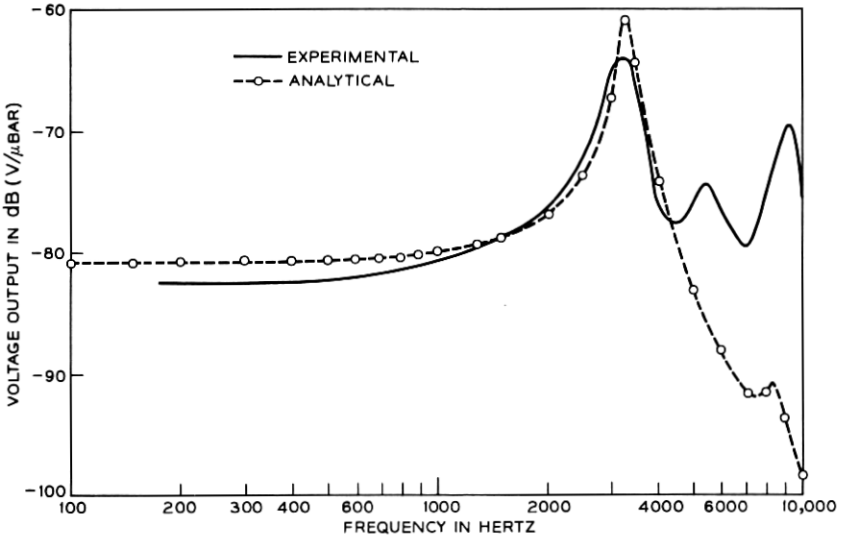

Fig. 7—Voltage output vs frequency, rubber: 50 percent cis-4 PBD, 50 percent SBR.

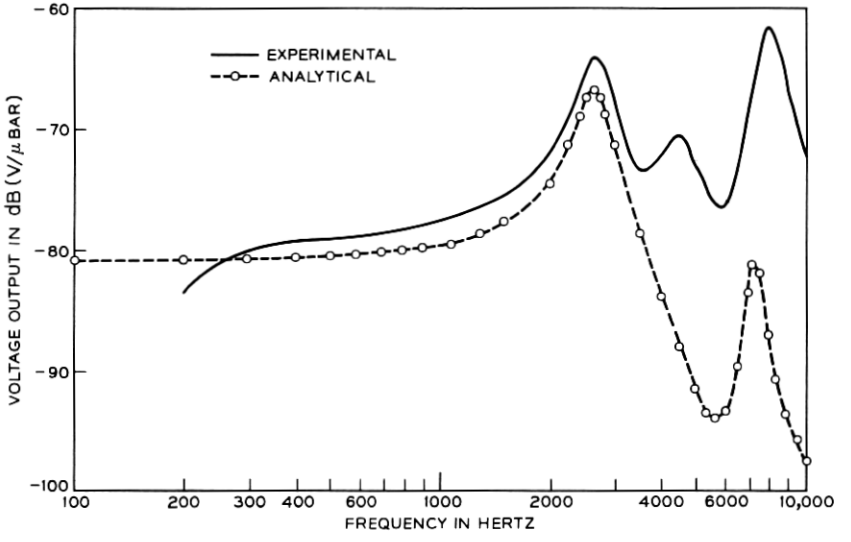

Fig. 8—Voltage output vs frequency, rubber: 75 percent cis-4 PBD, 25 percent CBT.

V. FINITE ELEMENT ANALYSIS

In order to understand the limitations of the lumped mechanical model of the rubber support, a finite element code[13] was exercised. The code was designed to dynamically analyze axisymmetric elastic solids subjected to arbitrary time-dependent loads and includes, as an option, the frequency and mode shape calculations for the solid. For this application, the ceramic was discretized into eighteen plate bending elements and the conical washers were discretized into three successively finer grids, with the most dense grid containing 92 quadrilateral continuum elements. All materials were treated as elastic—the absolute value of the complex extensional modulus of the rubber was used—and Poisson's ratio was chosen to be either 0.45 or 0.49.

A modal survey was then conducted for varying values of rubber extensional modulus. The four lowest resonant frequencies and their corresponding mode shapes were calculated for each modulus value. Typical results are shown in Figs. 9a–9d. These figures portray the influence of the rotatory inertia of the cantilevered frustum, which vibrates either in-phase or out-of-phase with the outer edge rotation of the ceramic. Note that the out-of-phase modes, Figs. 9a and 9c, are not strongly piezoelectrically active, whereas the in-phase modes, Figures 9b and 9d indicate substantial edge rotation with reference to central deflection.

A composite plot of all the results obtained from the modal survey is shown in Fig. 10. This plot correlates well with the experimental results of Figs. 7 and 8. Note that the results are only slightly dependent on the value of Poisson's ratio and on the discretization.

VI. CONCLUSIONS

With the knowledge gained from these three phases of analysis, a coherent set of design conclusions can be drawn. These recommendations fall into two categories: (*i*) rubber material selection and (*ii*) conical washer design modification. In Figs. 11 and 12 the response variation of the ceramic transducer and its rubber supports is shown, as a function of environmental temperature, for the two different rubbers.[14,15] Clearly, the rubber modulus is increasing too rapidly and the loss tangent is not holding an adequate value at the lower temperatures. In addition, the rotatory inertia of the unconstrained rubber is creating intolerable amplitude levels at the higher frequencies. In a recent investigation,[16] block copolymers cast from different solvents seemed to yield dynamic mechanical properties with desirable damping

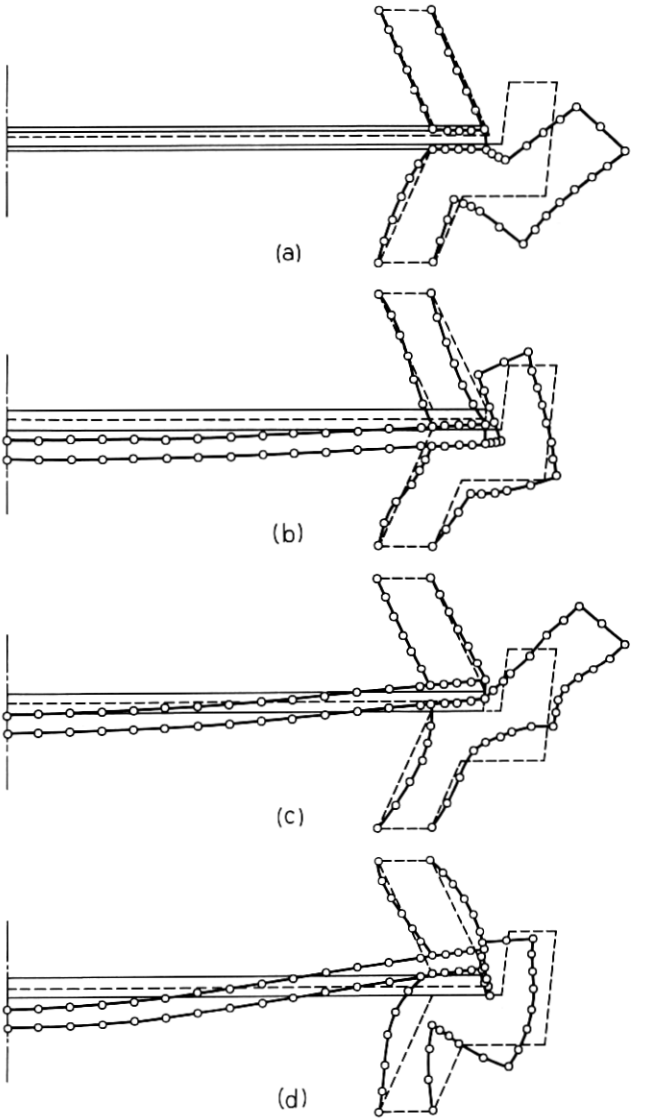

Fig. 9a—Resonant mode shape, $f_0 = 2250$ Hertz, $E_R = 40 \times 10^6$ dynes/cm^2.

Fig. 9b—Resonant mode shape, $f_0 = 2700$ Hertz, $E_R = 40 \times 10^6$ dynes/cm^2.

Fig. 9c—Resonant mode shape, $f_1 = 5400$ Hertz, $E_R = 60 \times 10^6$ dynes/cm^2.

Fig. 9d—Resonant mode shape, $f_2 = 8500$ Hertz, $E_R = 80 \times 10^6$ dynes/cm^2.

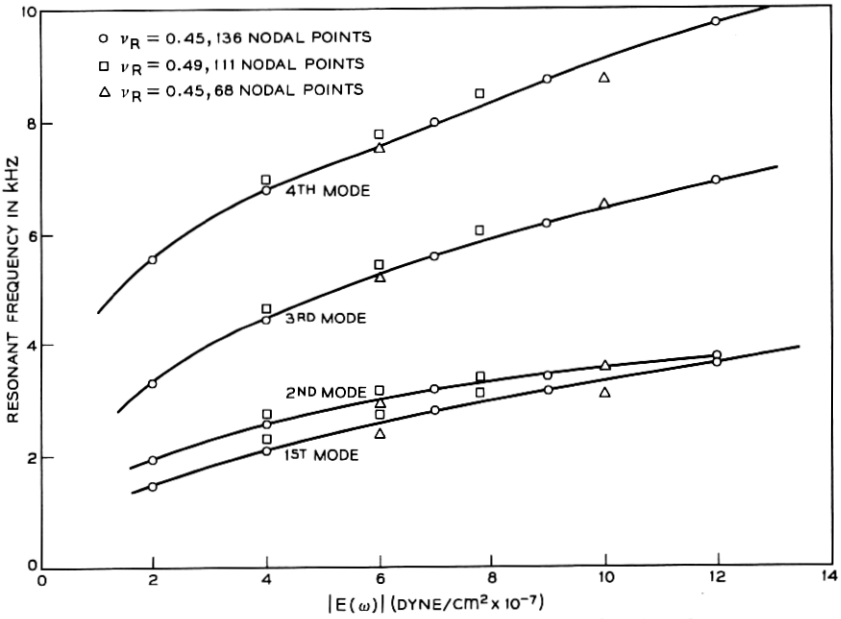

Fig. 10—Finite element frequencies vs rubber extensional modulus.

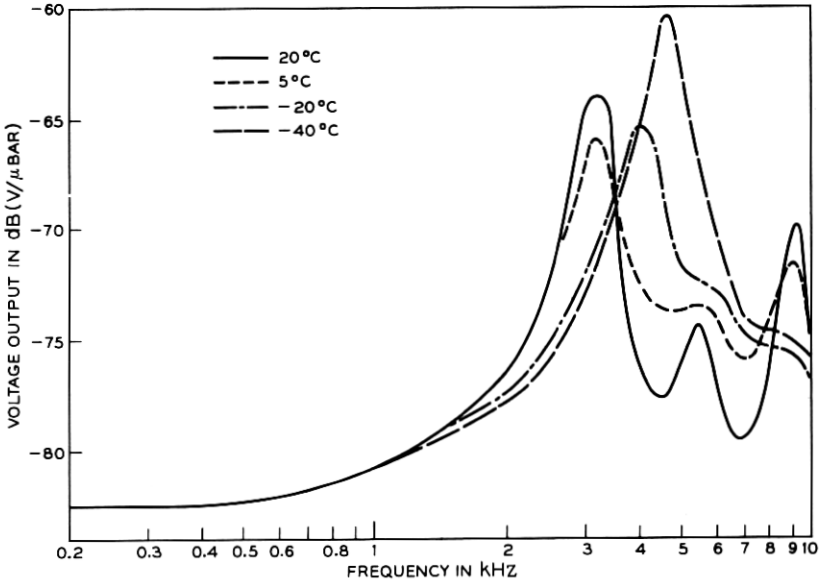

Fig. 11—Frequency response vs temperature change, rubber: 50 percent PBD, 50 percent SBR.

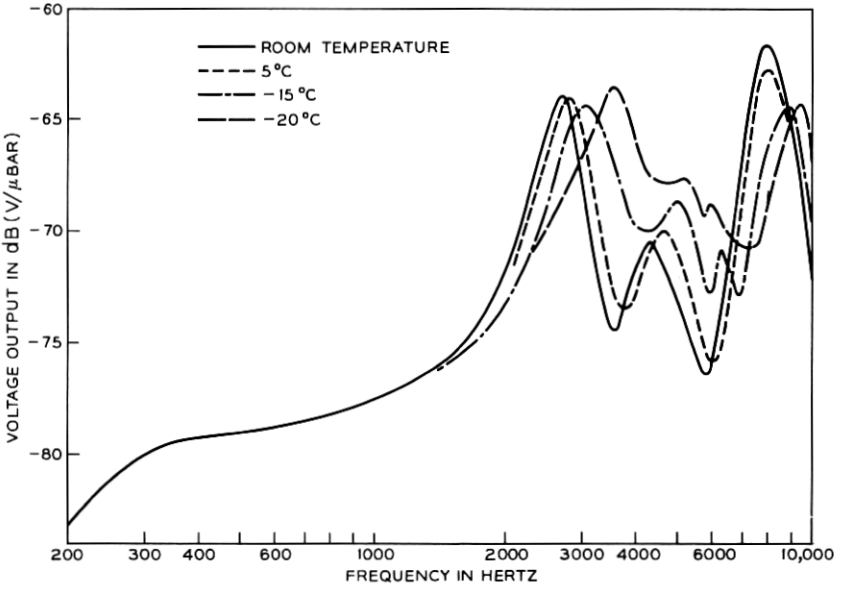

Fig. 12—Frequency response vs temperature change, rubber: 75 percent PBD, 25 percent CBT.

characteristics and relatively stable stiffness. Because of the dual transition (see Fig. 13), a styrene-butadiene-styrene block copolymer, obtained from solutions in carbon tetrachloride (c), toluene (T), ethyl acetate (E), and methyl ethyl ketone (M), has a sufficiently high loss tangent over a 200°C temperature range and also has a relatively constant modulus over a 130°C range. If the modulus is too high over this range, the washer design can be modified—thinner and taller cross section—to achieve nominal stiffness. A material tailoring program might produce a rubber which will help the transducer meet the design template.

In addition to the improvement of rubber mechanical properties, the washer design should be altered in order to decrease, substantially, the rotatory inertia of the unrestrained cantilever section. One possibility is shown in Fig. 14. An inverted vee-shaped design is depicted for the bottom washer that has three salient features: (*i*) a thinner cross section in order to maintain the modulus/stiffness ratio; (*ii*) restraint of the cantilevered section; and (*iii*) a seating lip to aid in fabrication of the transducer.

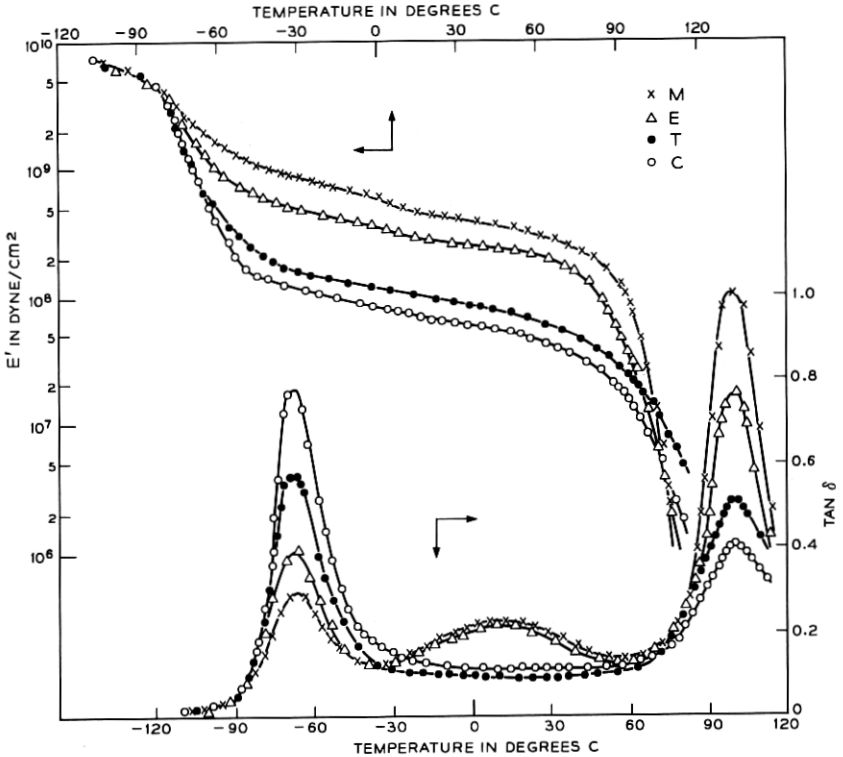

Fig. 13—E' and tan δ vs temperature.

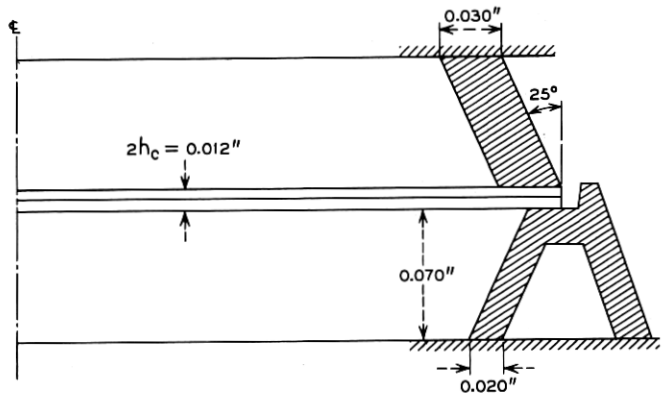

Fig. 14—Modified conical washer design.

VII. ACKNOWLEDGMENTS

The authors would like to acknowledge the design work and measurements of H. W. Bryant and T. C. Austin. They would also like to acknowledge the efforts of D. L. Loan and W. F. Moore for their work on the rubber materials.

In particular, they would like to thank W. D. Goodale for his very professional coordination of the project.

APPENDIX

Voltage Output Calculation

The voltage output of the bimorph ceramic microphone is calculated from the strain field under the following assumptions.

The significant contributions to the component of the electric field, $E_z(r)$, perpendicular to the midplane of the plate are generated by the two strain components ϵ_{rr} and $\epsilon_{\theta\theta}$. This assumes that the electric displacement field is negligible. Hence

$$\begin{aligned} \mathbf{Z}\cdot\mathbf{E}(r) = E_z(r) &= \mathbf{Z}\cdot(-\mathbf{h}\cdot\mathbf{S} + \boldsymbol{\beta}\cdot\mathbf{D}) \\ &\doteq -h_{12}\epsilon_{12} - h_{13}\epsilon_{13}\,, \end{aligned} \tag{18}$$

where $\mathbf{Z}$ is the unit normal vector to the plate, $\mathbf{h}$ the piezoelectric tensor relating strain, $\mathbf{S}$, to electric field, and $\boldsymbol{\beta}$ the electric displacement field, $\mathbf{D}$, to electric field.[17] However, for a ceramic poled in the $\mathbf{Z}$ direction, $h_{13} = h_{12}$; hence,

$$\begin{aligned} E_z(r) &= -h_{13}(\epsilon_{12} + \epsilon_{13}) \\ &= -h_{13}(\epsilon_{rr} + \epsilon_{\theta\theta}). \end{aligned} \tag{19}$$

From thin-plate theory, the strain term is given in terms of the midplane displacement, $w(r)$, by the expression

$$\epsilon_{rr} + \epsilon_{\theta\theta} = -z\left[\frac{1}{r}\frac{d}{dr}\left(r\frac{dw}{dr}\right)\right]; \tag{20}$$

thus

$$E_z(r) = +zh_{13}\left[\frac{1}{r}\frac{d}{dr}\left(r\frac{dw}{dr}\right)\right]. \tag{21}$$

The average electric field over the plated area is given by

$$E_{ave} = \frac{1}{\pi r_p^2}\int_0^{r_p}\int_0^{2\pi} E_z(r) r\, dr\, d\theta, \tag{22}$$

where r_p is the electroded radius.

Substitution of (21) in (22) yields

$$E_{\text{ave}} = \frac{2zh_{13}}{r_p^2}\left(r\frac{dw}{dr}\right)_{r=r_p}. \tag{23}$$

The potential difference across one plate is therefore given by the line integral $\int_0^{h_c} E_{\text{ave}}\, dz$, but, since the two plates are series connected, the total voltage is given by

$$V(f) = \frac{2h_{13}}{r_p^2} h_c^2 r\left(\frac{dw}{dr}\right)_{r=r_p}, \tag{24}$$

where h_c is the thickness of one ceramic disk, and $h = 2h_c$ the total thickness.

REFERENCES

1. Bryant, H. W., "Telephone Transmitter Designs Having Ceramic Transducers," unpublished work.
2. O'Bryan, H. M., Jr., and Bryant, H. W., "Ceramic Assemblies for Microphones," unpublished work.
3. Austin, T. C., and Herson, R. J., "Response Shaping of Transducer by Optimization of Housing Geometry," unpublished work.
4. Ferry, J. D., *Viscoelastic Properties of Polymers*, Second Edition, New York: John Wiley and Sons, Inc., 1970, p. 145.
5. Ibid., pp. 292–351.
6. Daane, J. H., private communication.
7. Ferry, loc. cit., p. 307.
8. Timoshenko, S., and Woinowsky-Krieger, S., *Theory of Plates and Shells*, Second Edition, New York: McGraw-Hill Book Company, 1959, pp. 344–346.
9. Rajappa, N. R., "Free Vibration of Rectangular and Circular Orthotropic Plates," AIAA J., *1*, May 1963, pp. 1194–1195.
10. Hilyard, N. C., "Effective Mass of Bonded Rubber Blocks," J. Acoust. Soc. Amer., *47*, 1969, pp. 1463–1465.
11. Schapery, R. A., "Approximate Methods of Transform Inversion for Viscoelastic Stress Analysis," Proc. Fourth U. S. Nat. Conf. Appl. Mech., June 1961, pp. 1075–1085.
12. Fung, Y. C., *Foundations of Solid Mechanics*, Englewood Cliffs, N. J.: Prentice-Hall, Inc., 1965, pp. 25–28.
13. Ghosh, S., and Wilson, E. L., "Dynamic Stress Analysis of Axisymmetric Structures Under Arbitrary Loading," Report No. *EERC 69–10*, Earthquake Engineering Research Center, University of California, Berkeley, September 1969.
14. Austin, T. C., private communication.
15. Bryant, H. W., private communication.
16. Miyamoto, T., Kodama, K., and Shibayama, K., "Structure and Properties of a Styrene-Butadiene-Styrene Block Copolymer," J. Polymer Sci. A-2, *8*, 1970, pp. 2095–2103.
17. Berlincourt, D. A., Curran, D. R., and Jaffe, H., "Piezoelectric and Piezomagnetic Materials and Their Function in Transducers," in *Physical Acoustics*, Vol. IA, edited by W. P. Mason, New York: Academic Press, 1964.